

Geophysical Research Letters®



RESEARCH LETTER

10.1029/2025GL117582

Key Points:

- Stronger North Atlantic cooling in response to volcanic eruption clusters in glacial climates
- This response depends on pre-existing upper-ocean conditions in the subpolar North Atlantic, leading to model-dependent results
- For our models and chosen eruption parameters, volcanic eruption clusters alone may be insufficient to cause millennial-scale cooling

Supporting Information:

Supporting Information may be found in the online version of this article.

Correspondence to:

D. Dutta,
dd643@cam.ac.uk

Citation:

Dutta, D., Hopcroft, P. O., Andreasen, L. S., Aubry, T. J., Timmreck, C., Zanchettin, D., et al. (2025). State-dependent North Atlantic response to volcanic eruption clusters. *Geophysical Research Letters*, 52, e2025GL117582. <https://doi.org/10.1029/2025GL117582>

Received 12 JUN 2025

Accepted 23 JUL 2025

Author Contributions:

Conceptualization: Deepashree Dutta, Peter O. Hopcroft, Thomas J. Aubry, Claudia Timmreck, Davide Zanchettin, Francesco Muschitiello

Data curation: Deepashree Dutta, Laurits S. Andreasen, Thomas J. Aubry

Formal analysis: Deepashree Dutta

Funding acquisition:

Francesco Muschitiello

Investigation: Deepashree Dutta, Laurits S. Andreasen

Methodology: Deepashree Dutta, Peter O. Hopcroft, Thomas J. Aubry, Francesco Muschitiello

Project administration:








Deepashree Dutta

Resources: Peter O. Hopcroft, Claudia Timmreck

© 2025. The Author(s).

This is an open access article under the terms of the [Creative Commons Attribution License](#), which permits use, distribution and reproduction in any medium, provided the original work is properly cited.

State-Dependent North Atlantic Response to Volcanic Eruption Clusters

Deepashree Dutta^{1,2,3} , Peter O. Hopcroft³ , Laurits S. Andreasen⁴ , Thomas J. Aubry^{5,6} , Claudia Timmreck⁷ , Davide Zanchettin⁸ , Xu Zhang⁹ , and Francesco Muschitiello^{1,2}

¹Department of Geography, University of Cambridge, Cambridge, UK, ²Centre for Climate Repair at Cambridge, Department of Applied Mathematics and Theoretical Physics, University of Cambridge, Cambridge, UK, ³School of Geography, Earth and Environmental Sciences, University of Birmingham, Birmingham, UK, ⁴School of Culture and Society - Department of Archeology and Heritage Studies, Aarhus University, Aarhus, Denmark, ⁵Department of Earth and Environmental Sciences, University of Exeter, Penryn, UK, ⁶Now at Department of Earth Sciences, University of Oxford, Oxford, UK, ⁷Max-Planck-Institute for Meteorology, Hamburg, Germany, ⁸Department of Environmental Sciences, Informatics and Statistics, University Ca' Foscari of Venice, Mestre, Italy, ⁹British Antarctic Survey, Cambridge, UK

Abstract Paleoclimate reconstructions suggest that clusters of volcanic eruptions may trigger sustained cooling events, but the underlying mechanisms and their potential dependence on the mean climate state remain poorly understood. Here, we investigate the climate response to an idealized eruption cluster using two coupled climate models under fully glacial, deglacial, and pre-industrial conditions. While the global mean temperature responses are largely climate-state independent, North Atlantic cooling is stronger under glacial conditions, especially in the Hadley Centre Model HadCM3. This response is primarily driven by a sustained weakening of the Atlantic Meridional Overturning Circulation due to increased surface buoyancy and sea-ice extent. However, the magnitude and duration of this response vary with climate state and model, due to differences in upper-ocean stability, convection zones, and sea-ice cover. Our results suggest that while volcanic clusters can induce intense cooling, they alone cannot sustain Younger Dryas-like climate shifts.

Plain Language Summary Paleoclimate reconstructions suggest that volcanic eruptions occurring in close succession, known as a volcanic eruption cluster, may trigger prolonged cooling events. However, the physical mechanisms driving this potential response remain unclear. The effect of the background climate (i.e., mean temperature, sea-ice cover, ocean-atmosphere circulation etc.) is also poorly understood. Here, we examine the climate response to an idealized volcanic eruption cluster using the Hadley Centre Coupled Model (HadCM3) and the Max Planck Institute Earth System Model under fully glacial, deglacial, and pre-industrial conditions. We find that the climate response to a volcanic eruption cluster depends not only on the mean state of the climate, but also on model characteristics, including the representation of upper-ocean temperature and salinity, the location and strength of deep convection sites, and sea-ice extent. Our results show that the global mean temperature responses are largely independent of the mean climate state in both models, but the response in the North Atlantic is highly model dependent. HadCM3 shows a stronger and more persistent cooling in the North Atlantic in already cold climates. Overall, for the volcanic cluster in the two models used in our study, volcanic forcing alone is not sufficient to sustain a millennial-scale cooling event.

1. Introduction

Volcanic eruptions are a key driver of natural climate variability on annual to multi-decadal timescales (Marshall et al., 2022; Myhre et al., 2013). Volcanic forcing is primarily due to the temporary enhancement of the stratospheric aerosol layer after major explosive eruptions and its main direct climatic consequence is short-term (5–10 years) post-eruption global surface cooling (Cole-Dai, 2010; Timmreck, 2012). This cooling can affect surface pressure and large-scale atmospheric circulation patterns, and lead to changes in upper-ocean conditions (Chen et al., 2022; Mignot et al., 2011; Zanchettin et al., 2012).

Beyond these immediate effects, volcanic eruptions can trigger multidecadal to centennial scale changes in the high-latitude ocean-atmosphere-cryosphere system, particularly in the North Atlantic (Miller et al., 2012; Neukom et al., 2019; Schleussner & Feulner, 2013; Zhong et al., 2011). However, the evolution of the North Atlantic following eruptions is highly uncertain, as it depends not only on eruption characteristics but also on background and initial ocean states (Zanchettin et al., 2013). While post-eruption sea surface temperature (SST) cooling and

Supervision: Peter O. Hopcroft,

Francesco Muschitiello

Visualization: Deepashree Dutta

Writing – original draft:

Deepashree Dutta

Writing – review & editing:

Deepashree Dutta, Peter O. Hopcroft,

Laurits S. Andreasen, Thomas J. Aubry,

Claudia Timmreck, Davide Zanchettin,

Xu Zhang, Francesco Muschitiello

enhanced ocean-to-atmosphere heat loss generally strengthen the Atlantic Meridional Overturning Circulation (AMOC), the long-term response is influenced by multiple interacting factors (Bilbao et al., 2024). Changes in subpolar gyre (SPG) dynamics, sea-ice expansion limiting ocean-atmosphere interaction, and variations in upper-ocean salinity and stability can all modulate AMOC, potentially shifting the upper-ocean state in the North Atlantic (Lehner et al., 2013; Moreno-Chamorro et al., 2017).

Volcanic eruptions occurring in close succession—i.e., a volcanic eruption cluster—may instigate a more profound influence on the long-term climate. Reconstruction (Helama et al., 2021; Kobashi et al., 2017) and modeling (van Dijk et al., 2022, 2024) studies focusing on the last millennium suggest that such clusters may have triggered a persistent shift in subpolar North Atlantic ocean temperatures and dynamical processes. Furthermore, volcanic reconstructions from Greenland and Antarctic ice-core records demonstrate synchronicity between eruptions and abrupt North Atlantic climate shifts, with a potential role for a cluster of eruptions during the Younger-Dryas (Abbott et al., 2021; Sigl et al., 2022; Svensson & Lohmann, 2022). The mean-state conditions during these past climates, such as global mean temperature, sea-ice extent, and greenhouse gas concentrations were very different from today's, thus the nature of the physical processes and amplifying feedbacks determining the response of the North Atlantic to volcanic eruptions could also have differed.

Modeling studies indicate that the state of the climate system influences both the stratospheric volcanic aerosol forcing (Aubry et al., 2019, 2021) and the climate response to the forcing (Fasullo et al., 2017; Hopcroft et al., 2018). Similarly, using ice core data spanning 12,000–60,000 years, Lohmann et al. (2024) reported a stronger cooling in Greenland following volcanic eruptions occurring under glacial conditions compared to the largest eruptions during the Common Era. Further highlighting the potential of strong volcanic eruptions to trigger or amplify abrupt climate shifts, paleoclimate reconstructions from the last glacial and deglaciation indicate that volcanic clusters often preceded cold stadials (Lin et al., 2023; Svensson et al., 2020).

Using ice core records, Abbott et al. (2021) suggested that a cluster of strong volcanic eruptions between 13,200 and 12,800 years ago may have triggered the Younger Dryas, a ~1,300-year-long abrupt cooling event. To our knowledge this hypothesis has not been tested with coupled climate models. Using a variable-magnitude volcanic history, Ellerhoff et al. (2022) revealed the potential of the background climate to significantly affect regional responses to volcanic forcing, especially due to state-dependent sea-ice changes; however, the underlying physical processes and the role of such state dependencies in determining post-eruption climate response remain unknown. Building on these studies, we conducted idealized volcanic eruption cluster experiments using the Hadley Centre Coupled Model Version 3 (HadCM3, Valdes et al., 2017) and Max Planck Institute Earth System Model (MPI-ESM-1.2-LR, Mauritsen et al., 2019) under Last Glacial Maximum (LGM), 12,000 years before present (12 kyr) and pre-industrial (PI) conditions to assess how background climate influences long-term post-eruption SST and sea-ice responses in the North Atlantic. We also integrate additional HadCM3 experiments with high-latitude Northern Hemisphere eruption clusters to examine how eruption latitude influences climate responses. Finally, we aim to identify the physical processes driving long-term changes in the North Atlantic.

2. Materials and Methods

2.1. Climate Models

The coupled ocean-atmosphere general circulation model HadCM3, used here for its computational efficiency, is run with the atmosphere (Pope et al., 2000) and ocean (Gordon et al., 2000) components at horizontal resolutions of $3.75^\circ \times 2.5^\circ$ and $1.25^\circ \times 1.25^\circ$, with 19 and 20 vertical levels, respectively. The extent and elevation of ice sheets are imposed as boundary conditions due to the lack of an interactive land-ice component in HadCM3. We used land-ice and sea level reconstructions based on the ICE-6G_C model (Peltier et al., 2015).

MPI-ESM-1.2-LR (hereafter MPI-ESM) is run with its atmospheric component ECHAM6 (Stevens et al., 2013) with a $1.86^\circ \times 1.86^\circ$ horizontal resolution and 47 vertical levels extending up to 0.01 hPa, and the ocean component MPIOM with a 1.5° horizontal resolution and 64 vertical levels (Jungclauss et al., 2013). Like HadCM3, the ICE-6G_C boundary conditions are prescribed in PI and LGM configurations of MPI-ESM. The newly adopted Allerød-like configuration for the 12 kyr experiments is described in Supporting Information S1.

2.2. Volcanic Forcing

We used an idealized volcanic cluster roughly based on Abbott et al. (2021), consisting of four exceptionally strong eruptions separated by 25-year intervals, each with an injection of 100 Tg S. The subpolar North Atlantic shows strong internal variability (Yeager & Danabasoglu, 2014); therefore, we chose a volcanic forcing higher than Abbott et al. (2021) to obtain a sufficiently high signal-to-noise ratio.

Monthly varying aerosol optical properties were generated using the reduced-complexity volcanic aerosol forcing model EVA-H (Aubry et al., 2020). EVA_H produces latitude, altitude, and wavelength dependent aerosol optical properties in response to prescribed volcanic sulfur injections. It was calibrated using a combination of satellite observations and interactive stratospheric aerosol model simulations, with the latter accounting for proportionally smaller forcing for large SO₂ injections (Metzner et al., 2014; Timmreck et al., 2010). We used eruption dates of April 1 for each eruption. To distinguish the impacts of the Northern Hemisphere tropical and high-latitude eruption clusters, two sets of forcing and corresponding climate model experiments were conducted by prescribing eruptions at 5°N and 50°N (Figure S1 in Supporting Information S1). There is a rapid increase in stratospheric aerosol optical depth (SAOD) across all latitude bands immediately after each eruption, reaching a maximum at the beginning of the second year. This is followed by an exponential decay over the next 4–5 years before SAOD returns to pre-volcanic levels. The 5°N eruption distributes SAOD evenly across both hemispheres, while the 50°N eruption mainly concentrates it in the northern high-latitudes.

MPI-ESM uses a zonally symmetric, depth-varying forcing at each latitude band, accounts for longwave radiation absorption by volcanic aerosols, and calculates their reflectivity at multiple shortwave radiation wavelengths (Stevens et al., 2013). In contrast, HadCM3 only requires the SAOD at 550 nm across four equal-area latitude bands, accounting solely for shortwave forcing with crude latitudinal resolution and no vertical aerosol distribution (Jones et al., 2005).

2.3. Experiments

We integrate 500-year-long control experiments with HadCM3 using boundary conditions representative of the LGM, 12 kyr, and PI (Table S1 in Supporting Information S1). We perform a 10-member ensemble for each mean state and eruption location: (a) PI_5N, 12kyr_5N, and LGM_5N and (b) PI_50N, 12kyr_50N, and LGM_50N. The evolution of Northern Hemisphere high-latitude SSTs, sea-ice, and ocean circulation is sensitive to the preexisting state of the subpolar North Atlantic (Reintges et al., 2024; Zhong et al., 2011). Therefore, the initialization years for the 10-member ensemble of the volcanic experiments are sampled from the first 300 years of each control experiment to represent the high variability of subpolar North Atlantic SSTs (Figure S2 in Supporting Information S1). Each volcanic experiment is run for 200 years. To assess the long-term post-eruption responses, we focus on the 100-year period starting 10 years after the fourth eruption (model years 85–184 in Figure 1). Time-varying anomalies are calculated as the difference from the 200-year mean of the control experiments, with ensemble-mean results presented throughout this study.

The LGM, 12 kyr, and PI control experiments with MPI-ESM are integrated for 100 years. A five-member ensemble of the 5°N volcanic experiment is run for 200 years using randomly chosen initial conditions. Due to computational and storage limitations, we only conducted the 5°N experiment with MPI-ESM.

We define a SPG index as the spatially averaged barotropic streamfunction over 50°N–65°N and 10°W–60°W, with negative values indicating cyclonic circulation. The AMOC index is defined as the maximum AMOC poleward of 45°N as in Zhang et al. (2014) and surface buoyancy fluxes are calculated following Willeit et al. (2024).

Texts S2 and S3 in Supporting Information S1 provide details on different control experiments and compare model-simulated PI North Atlantic conditions with present-day observations.

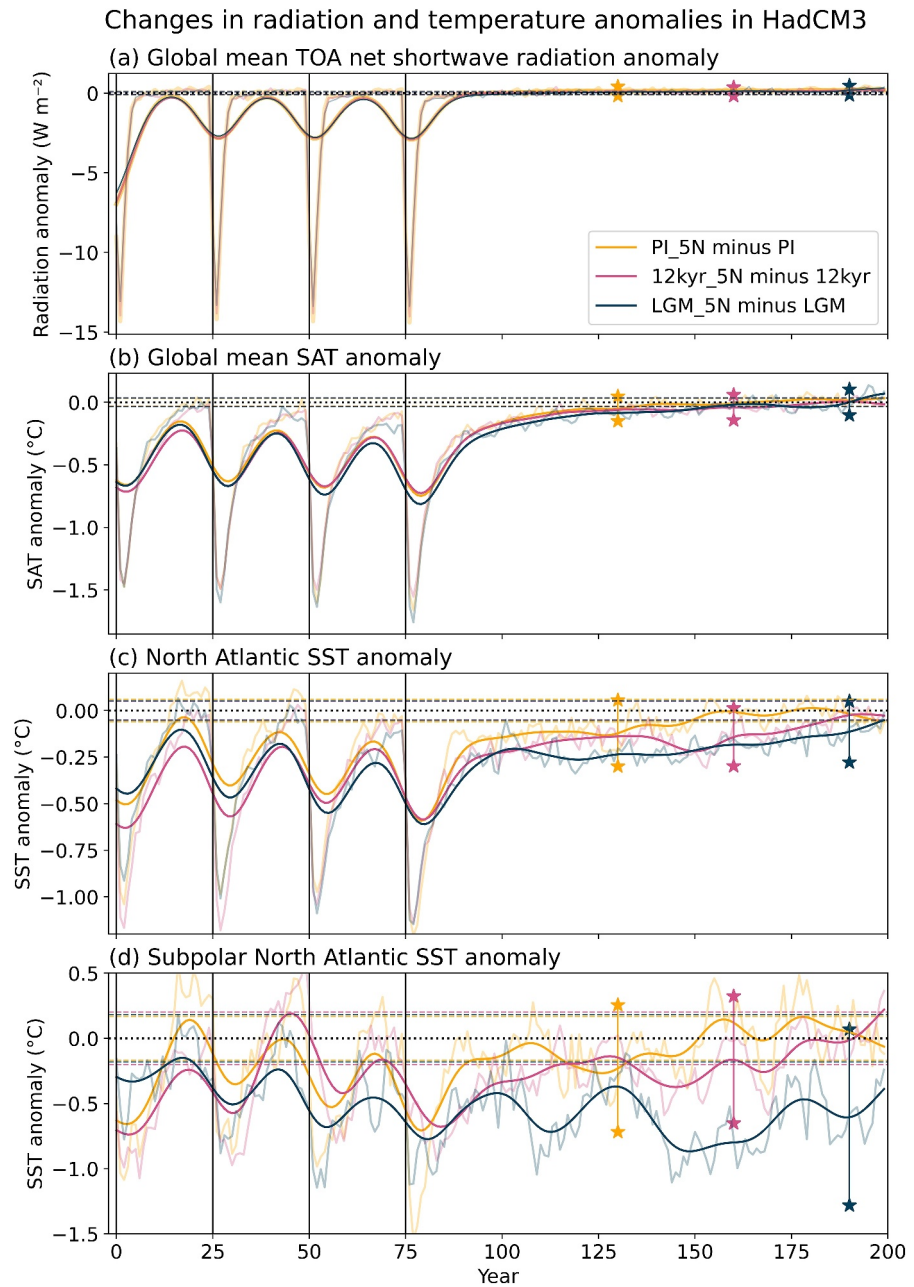


Figure 1. HadCM3 temporal evolution of (a) global mean top-of-atmosphere net shortwave radiation, (b) global mean surface air temperature, (c) North Atlantic sea surface temperature (SST) (0°N–60°N, 0°W–80°W), and (d) subpolar North Atlantic SST (50°N–60°N, 55°W–25°W) anomalies: PI_5N minus PI (yellow), 12kyr_5N minus 12kyr (pink), and LGM_5N minus LGM (blue). Thick solid lines, lighter solid lines, and horizontal dashed lines show the ensemble-means smoothed with a Gaussian filter (smoothing parameter of 5), yearly means, and standard deviations in the control simulations, respectively. Black vertical lines mark eruption timings, and the stars indicate standard deviation across the ensemble.

3. Results

3.1. Responses to the Tropical Eruption Cluster in HadCM3

3.1.1. Temperature Response

The increase in SAOD leads to a peak global mean top-of-atmosphere net shortwave radiation reduction of $\sim 14 \text{ W m}^{-2}$ (Figure 1a) immediately after each eruption. Correspondingly, net surface shortwave radiation decreases. These shortwave radiation anomalies gradually diminish within 5–6 years with reduction in SAOD.

The decrease in surface shortwave radiation triggers a global mean surface air temperature (SAT) cooling of up to $\sim 1.5^\circ\text{C}$ (Figure 1b). This cooling persists beyond the shortwave radiation anomaly and influences the temperature responses to subsequent eruptions. To analyze the residual cooling effects, we compare the annual mean SAT for the 10 years following each eruption with the 10-year average conditions preceding the eruption (Figures S3a–S3c in Supporting Information S1). This analysis shows that the small additional cooling after the second, third, and fourth eruptions (Figure 1b) results from the residual effects of earlier eruptions.

While the magnitude of the global SAT anomalies is similar across different boundary conditions, the background climate states strongly influence the North Atlantic SST responses, particularly in the subpolar regions (Figure 1). Following the eruption cluster, the magnitude of SST cooling is more intense in LGM_5N than in 12kyr_5N and PI_5N, with these differences becoming more pronounced over time. Additionally, the recovery period is longer in LGM_5N (Figures 1c and 1d). Higher internal variability in LGM may influence the post-eruption temperature response. The residual cooling effect of individual eruptions amplifies the total response (Figures S3g–S3i in Supporting Information S1), with mean subpolar SST anomalies remaining below approximately -0.5°C throughout the 100-year post-eruption period in LGM_5N (Figure 1d). We find similar basin-wide SST responses immediately after each eruption across the mean climate states (Figures S3d–S3f in Supporting Information S1). However, the magnitude and recovery time of the subpolar SST anomalies vary between these states, with no clear trend across the cluster (Figures S3g–S3i in Supporting Information S1).

The post-eruption 100-year mean upper-ocean temperature anomalies show significantly stronger cooling in LGM_5N compared to 12kyr_5N and PI_5N (Figures 2a–2c). Stronger anomalies occur along the western boundary, poleward of $\sim 40^\circ\text{N}$ in LGM_5N, promoting winter sea-ice expansion and ocean stratification. In contrast, temperature anomalies in 12kyr_5N and PI_5N are less pronounced across the North Atlantic.

In LGM_5N, convection sites shift southward, and the mixed layer depth (MLD) at the center decreases by $\sim 100 \text{ m}$ (Figure 2d), accompanied by an increase in sea-ice within the convection zone. Whereas, in 12kyr_5N, weak MLD reductions south of Greenland coincide with a slight increase in winter sea-ice fraction, and minimal MLD changes occur in PI_5N, with most anomalies not statistically significant (Figures 2d–2f).

3.1.2. Changes in Subpolar Gyre, Convection Zone, and AMOC Strength

The anomalies of the SPG strength, AMOC, meridional ocean heat transport, buoyancy fluxes, and sea-ice cover illustrate the complexity of the post-eruption ocean circulation responses in the North Atlantic (Figure 3). In general, the immediate ocean responses to eruptions are characterized by a rapid strengthening of the SPG, accompanied by enhanced poleward heat transport, increasing buoyancy fluxes in convective zones that drive a local sea-ice expansion, and a delayed strengthening of the AMOC. However, the timing and amplitude of post-eruption anomalies largely differ across experiments and between different eruptions within the same cluster.

Following the eruption cluster, we find a long-term strengthening of the SPG in LGM_5N. However, changes in the SPG and AMOC are decoupled, likely due to the relative locations of SPG in the western North Atlantic and the convection centre south of Iceland. Instead, buoyancy changes within the convection zone directly influence AMOC strength. The surface buoyancy flux within the convection zone gradually increases after the second eruption, leading to a long-term AMOC weakening trend in LGM_5N (Figures 3a and 3d). Generally, both a reduction in surface cooling and an increase in freshwater flux tend to increase buoyancy flux. In our experiments, changes in thermal flux play the dominant role in increasing buoyancy flux within the convection zone (Figure S4 in Supporting Information S1). The reductions in AMOC strength and poleward ocean heat transport result in surface cooling, promoting continuous sea-ice growth within the convection zone. This sea-ice expansion limits

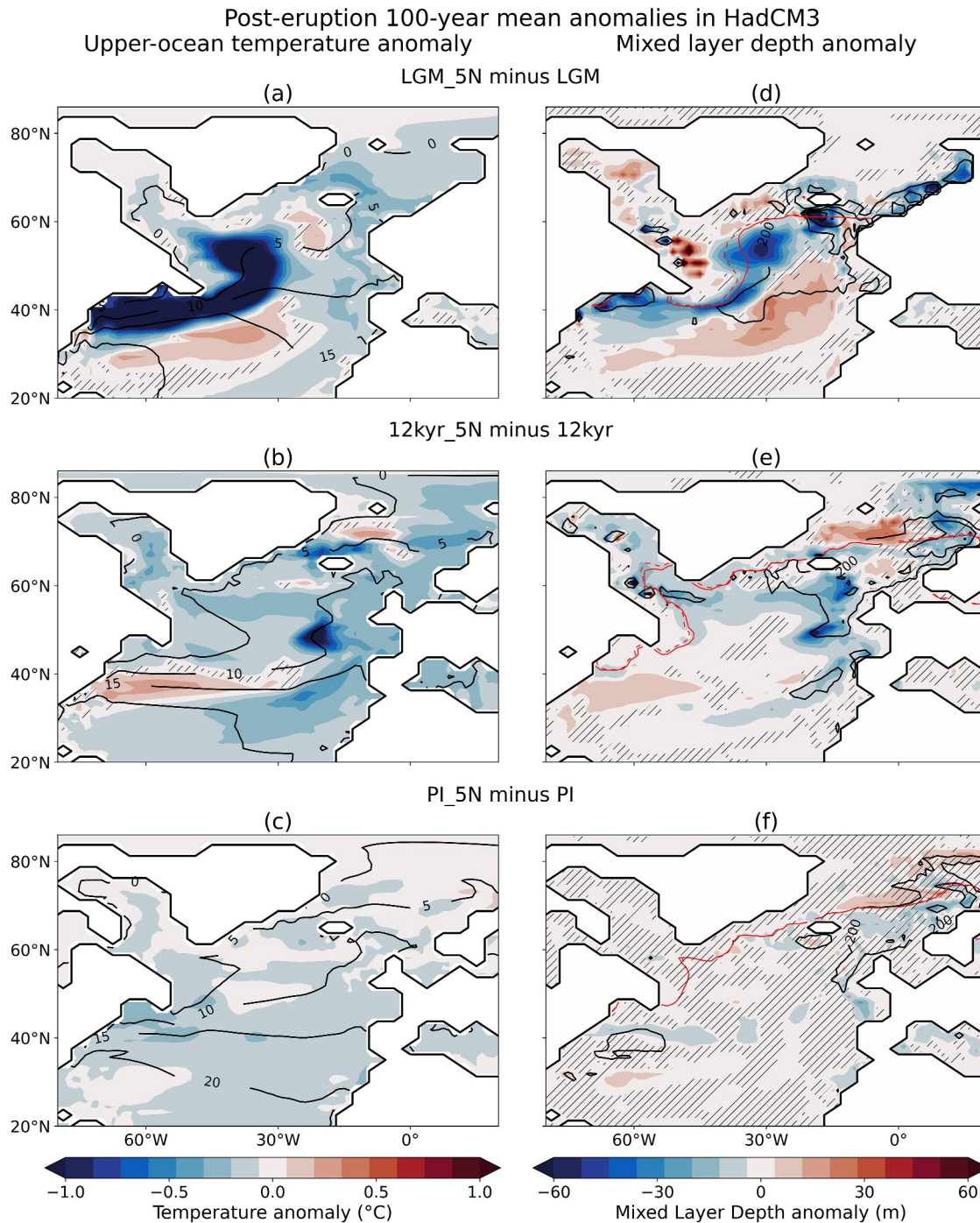


Figure 2. Ensemble-mean 100-year post-eruption annual mean 450 m averaged temperature anomalies in HadCM3: (a) LGM_5N minus LGM, (b) 12kyr_5N minus 12kyr, and (c) PI_5N minus PI. (d–f) Show winter-mean mixed layer depth (MLD) anomalies. The anomalies (color shading) are calculated as the difference between the 100-year mean temperature and MLD following the eruption cluster (years 85–184 in Figure 1) and the means of respective control periods. The black contours in panels (a–f) show temperature and MLD (>200 m) in the control experiments, with contour intervals of 5°C and 200 m, respectively. The red solid and dashed lines in panels (d–f) indicate 15% sea-ice fractions in the volcanic and control experiments. Hatching shows anomalies that are not significant at the 95% confidence level, based on a two-sided *t*-test.

air-sea flux exchange, reduces upper-ocean mixing, and weakens convection strength (Figures 2d–2f) while freshening surface waters. LGM_5N experiences a more pronounced AMOC weakening (>2 Sv) and requires a longer recovery period compared to both 12kyr_5N and PI_5N (Figures 3a–3c).

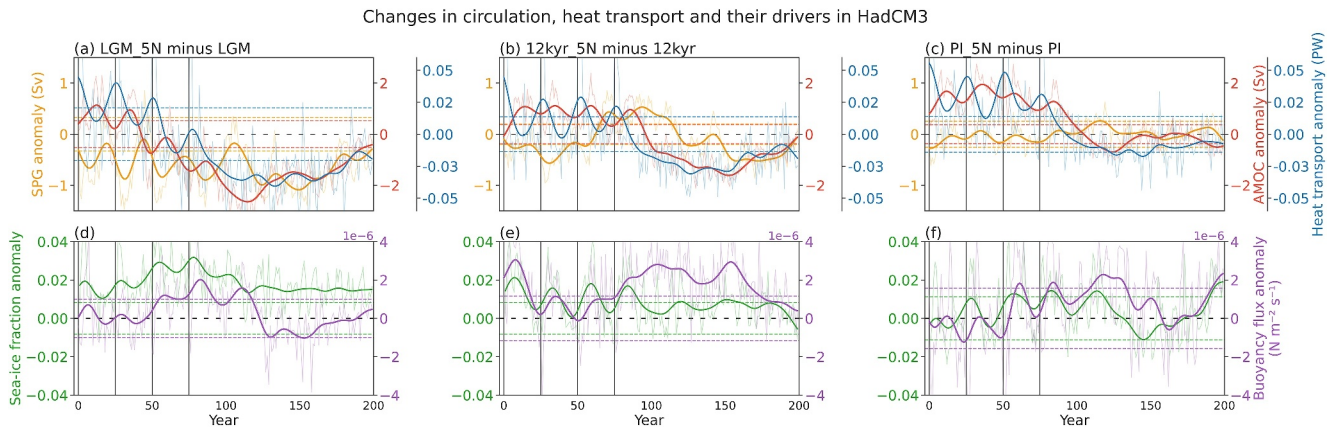


Figure 3. Factors influencing Atlantic Meridional Overturning Circulation (AMOC) in HadCM3: (a, d) LGM_5N minus LGM, (b, e) 12kyr_5N minus 12kyr, and (c, f) PI_5N minus PI. (a–c) Show the ensemble-mean subpolar gyre (orange), AMOC (red), and meridional ocean heat transport at 40°N over the North Atlantic (blue), while (d–f) display sea-ice fraction (green) and buoyancy flux (magenta) within the convection zone. The darker lines represent the ensemble-means smoothed with a Gaussian filter, while the lighter lines show annual mean values. Horizontal dashed lines indicate standard deviations in the control simulations, and vertical black lines mark the timing of eruptions.

3.2. Comparison Between HadCM3 and MPI-ESM

In similar 5°N experiments conducted with MPI-ESM, we find a slightly higher global mean shortwave radiation anomaly compared to HadCM3, likely due to differences in the treatment of stratospheric aerosols and radiation schemes in each model (Section 2.2). Despite this, the post-eruption 100-year mean global SST anomalies in both models show similar magnitudes (Figure 4a). However, in the North Atlantic, MPI-ESM shows smaller temperature anomalies in LGM_5N and 12kyr_5N compared to HadCM3, particularly over the subpolar regions. These SST differences are closely linked to the magnitude and persistence of AMOC changes in each model (Figure S5 in Supporting Information S1). Additionally, the spread in these anomalies is smaller in the MPI-ESM ensemble, likely due to its initial conditions having lower variability than those of HadCM3 (Figure S2 in Supporting Information S1).

The AMOC and poleward ocean heat transport anomalies are weaker (Figure 4b) in MPI-ESM compared to HadCM3, particularly in LGM_5N and 12kyr_5N. Differences in the representation of convection strengths and regions (Figures S6a–S6f in Supporting Information S1) give rise to these discrepancies between the models. In MPI-ESM, the upper ocean density in the North Atlantic is higher than in HadCM3, particularly along the eastern boundary (Figure S7 in Supporting Information S1). Moreover, across all boundary conditions, the climatological

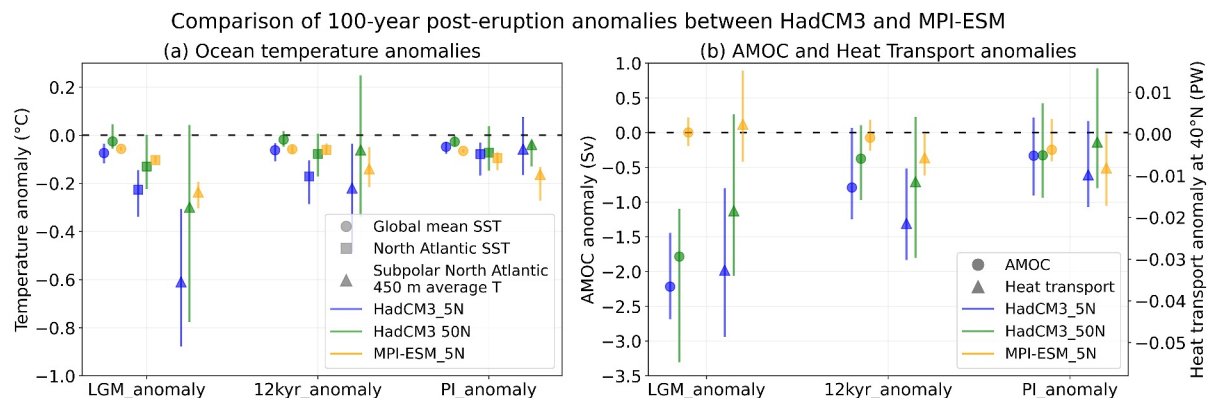


Figure 4. Ensemble-mean 100-year post-eruption annual mean (a) ocean temperature and (b) Atlantic Meridional Overturning Circulation (AMOC) and heat transport anomalies relative to the means of respective control simulations. Circular, square, and triangular markers in panel (a) represent global mean sea surface temperature (SST), North Atlantic SST, and the top 450 m average ocean temperature over the subpolar North Atlantic, respectively. In panel (b), circular and square markers denote anomalies of AMOC strength and ocean heat transport at 40°N over the North Atlantic. Blue and orange indicate HadCM3 and MPI-ESM results for the 5°N cluster, while green represents HadCM3 results for the 50°N cluster experiment.

deep convection in MPI-ESM is considerably greater in both spatial extent and depth than HadCM3 (Figure S6 in Supporting Information S1). In contrast, the AMOC in HadCM3 is driven by a localized region of strong mixing, which is partially covered by the winter sea-ice edge (defined as the 15% sea-ice concentration), particularly in LGM_5N. The proximity of these deep-water formation regions to the sea-ice edge suggests that AMOC strength in HadCM3 is more sensitive to small changes in sea-ice fraction within the convection zone than MPI-ESM. Therefore, even a small sea-ice increase within the convection zone can limit deep water formation and drastically reduce AMOC strength in HadCM3.

3.3. Responses to the High-Latitude Eruption Cluster in HadCM3

High-latitude eruptions in LGM_50N, 12kyr_50N, and PI_50N result in smaller global and North Atlantic 100-year post-eruption mean ocean temperature anomalies compared to tropical eruptions (Figure 4a). Despite showing a similar regional cooling pattern in the North Atlantic (Figure S8 in Supporting Information S1), the post-eruption upper-ocean temperature anomalies from the high-latitude cluster are consistently weaker than those from the tropical cluster across all climate states. Similarly, the AMOC and ocean heat transport responses are less pronounced in LGM_50N and 12kyr_50N compared to LGM_5N and 12kyr_5N (Figure 4b).

4. Discussions and Conclusions

Earlier studies suggested a link between volcanic eruption clusters and long-lasting cooling events, with the post-eruption climate response potentially varying based on the background climate (Miller et al., 2012; Zanchettin et al., 2013; Zhong et al., 2011). In line with the Volcanic forcing Model Intercomparison Project (Zanchettin et al., 2016), we examined the long-term response of the climate system to an idealized tropical eruption cluster and the associated physical processes, with a particular focus on the North Atlantic, using HadCM3 and MPI-ESM under LGM, 12 kyr and PI boundary conditions. We also assessed the influence of eruption latitude by conducting HadCM3 experiments with a volcanic eruption cluster in the Northern high latitudes. Our key findings are:

- Colder mean states result in stronger, longer-lasting North Atlantic cooling without affecting the global response

We find that post-eruption global mean shortwave radiation and temperature anomalies are largely similar across different boundary conditions in both models. However, on a regional scale, the response to volcanic forcing is state-dependent, particularly in the North Atlantic, consistent with earlier studies (Ellerhoff et al., 2022; Zanchettin et al., 2013). Despite identical volcanic forcing, the colder mean climate in LGM results in stronger North Atlantic cooling compared to PI and 12 kyr, particularly in HadCM3. This is in qualitative agreement with the ice-core-based study by Lohmann et al. (2024), which indicates that volcanic eruptions during glacial climates cause more pronounced cooling in northern high latitudes than during the Common Era. Our results also support the findings of van Dijk et al. (2024), highlighting the crucial role of ocean-sea-ice feedback in prolonged cooling events triggered by clustered volcanic eruptions. The differences in North Atlantic responses across different mean climates are mainly driven by variations in preexisting upper-ocean conditions, particularly the location, extent, and strength of convection sites in the subpolar North Atlantic.

- Strongly model-dependent North Atlantic climate response

HadCM3 and MPI-ESM show similar magnitudes of post-eruption global temperature anomalies, but MPI-ESM exhibits weaker cooling in the North Atlantic, particularly in the subpolar regions under LGM and 12 kyr. Post-eruption AMOC weakening in the models result from increased sea-ice and buoyancy in the convection zone. MPI-ESM generally recovers faster due to stronger convection over a larger area, while the more localized convection in HadCM3, makes it more sensitive to sea-ice changes, resulting in greater AMOC weakening and a longer recovery. These results suggest that the evolution of subpolar North Atlantic SST is influenced by biases in upper-ocean representations across climate models (Klockmann et al., 2020; Mehling et al., 2024; Reintges et al., 2024).

- Similar North Atlantic cooling patterns regardless of eruption location

Both tropical and high-latitude Northern Hemisphere eruption clusters induce remarkably similar SST, MLD, sea-ice response patterns in the North Atlantic. While the long-term responses remain largely independent of the

eruption latitude, the magnitude, and duration of these effects are weaker and shorter-lived for high-latitude eruption clusters.

These results support the possibility that volcanic clusters could trigger long-term cooling events. However, despite exceptionally strong eruptions in our experiments, AMOC and heat transport anomalies begin recovering within 100 years across boundary conditions. This suggests that for the chosen eruption cluster, volcanic forcing alone is insufficient to sustain a millennial-scale cooling event like the Younger Dryas in the two models. Therefore, other processes, such as changes in meltwater input or a more pronounced threshold transition, would be needed alongside eruption-induced cooling to trigger the transition to a stable cooling state.

Our results likely reflect the relatively high and intermediate AMOC stability in HadCM3 and MPI-ESM, respectively, as reported by Malmierca-Vallet et al. (2024). Their study showed that AMOC stability in climate model simulations of glacial periods is strongly influenced by North Atlantic sea-ice area, which also show significant model biases (Berdahl & Robock, 2013; SMIMIP, 2020). This suggests that models with lower AMOC stability may simulate prolonged AMOC weakening. Future studies using a larger model ensemble with a range of AMOC stability and improved representation of cryosphere-ocean interactive processes would help better constrain the climate response to volcanic forcing.

Additionally, for the same volcanic eruption intensity and sulfur injection magnitude, Aubry et al. (2019, 2021) demonstrate that the forcing would differ under different background climate conditions. Such effects, ignored in our study, could be simulated using climate models with interactive stratospheric aerosol modules. These efforts would refine our understanding of the physical processes driving long-term ocean-atmosphere-cryosphere responses, crucial for interpreting paleoclimate records and improving future climate projections.

Data Availability Statement

Check Valdes et al. (2017) for details on HadCM3. The MPI-ESM code is accessible from Model Development Team Max-Planck-Institut für Meteorologie (2024). Model output generated in this study is accessible from Dutta and Andreassen (2025).

Acknowledgments

We thank Marie Kapsch and Uwe Mikolajewicz for their assistance with the MPI-ESM model. DD is supported by the Arnell funding from the Centre for Climate Repair, POH by NERC (NE/X000869/1, NE/X000567/1, and NE/Z000025/1), LA by ERC project CLIOARCH (817564), CT by the Deutsche Forschungsgemeinschaft Research Unit VolImpact (FOR2820 (Grant 398006378)), TJA by the CMIP International Project Office (4000136906) and the European Space Agency project “Volcanic forcing for CMIP” (4000145911/24/I-LR), and FM by a NERC Discovery Science Grant (NE/W006243/1). This work used computational resources from the Birmingham Environment for Academic Research (BEAR HPC and RDS) and the Deutsches Klimarechenzentrum granted by its Scientific Steering Committee (WLA) under project 1251.

References

- Abbott, P. M., Niemeier, U., Timmreck, C., Riede, F., McConnell, J. R., Severi, M., et al. (2021). Volcanic climate forcing preceding the inception of the Younger Dryas: Implications for tracing the Laacher see eruption. *Quaternary Science Reviews*, 274, 107260. <https://doi.org/10.1016/j.quascirev.2021.107260>
- Aubry, T. J., Cerminara, M., & Jellinek, A. M. (2019). Impacts of climate change on volcanic stratospheric injections: Comparison of 1-D and 3-D plume model projections. *Geophysical Research Letters*, 46(17–18), 10609–10618. <https://doi.org/10.1029/2019GL083975>
- Aubry, T. J., Staunton-Sykes, J., Marshall, L. R., Haywood, J., Abraham, N. L., & Schmidt, A. (2021). Climate change modulates the stratospheric volcanic sulfate aerosol lifecycle and radiative forcing from tropical eruptions. *Nature Communications*, 12(1), 4708. <https://doi.org/10.1038/s41467-021-24943-7>
- Aubry, T. J., Toohey, M., Marshall, L., Schmidt, A., & Jellinek, A. M. (2020). A new volcanic stratospheric sulfate aerosol forcing emulator (EVA_H): Comparison with interactive stratospheric aerosol models. *Journal of Geophysical Research: Atmospheres*, 125(3), e2019JD031303. <https://doi.org/10.1029/2019JD031303>
- Berdahl, M., & Robock, A. (2013). Northern hemispheric cryosphere response to volcanic eruptions in the paleoclimate modeling intercomparison project 3 last millennium simulations. *Journal of Geophysical Research: Atmospheres*, 118(22), 12359–12370. <https://doi.org/10.1002/2013JD019914>
- Bilbao, R., Ortega, P., Swingedouw, D., Hermanson, L., Athanasiadis, P., Eade, R., et al. (2024). Impact of volcanic eruptions on CMIP6 decadal predictions: A multi-model analysis. *Earth System Dynamics*, 15(2), 501–525. <https://doi.org/10.5194/esd-15-501-2024>
- Chen, K., Ning, L., Liu, Z., Liu, J., Yan, M., Sun, W., et al. (2022). Modulating and resetting impacts of different volcanic eruptions on north Atlantic SST variations. *Journal of Geophysical Research: Atmospheres*, 127(16), e2021JD036246. <https://doi.org/10.1029/2021JD036246>
- Cole-Dai, J. (2010). Volcanoes and climate. *Wiley Interdisciplinary Reviews: Climate Change*, 1(6), 824–839. <https://doi.org/10.1002/wcc.76>
- Dutta, D., & Andreassen, L. (2025). HadCM3 and MPI-ESM output from idealised volcanic cluster experiments [Dataset]. *figshare*. <https://doi.org/10.6084/m9.figshare.29596460.v1>
- Ellerhoff, B., Kirschner, M. J., Ziegler, E., Holloway, M. D., Sime, L., & Rehfeld, K. (2022). Contrasting state-dependent effects of natural forcing on global and local climate variability. *Geophysical Research Letters*, 49(10), e2022GL098335. <https://doi.org/10.1029/2022GL098335>
- Fasullo, J. T., Tomas, R., Stevenson, S., Otto-Bliesner, B., Brady, E., & Wahl, E. (2017). The amplifying influence of increased ocean stratification on a future year without a summer. *Nature Communications*, 8(1), 1236. <https://doi.org/10.1038/s41467-017-01302-z>
- Gordon, C., Cooper, C., Senior, C. A., Banks, H., Gregory, J. M., Johns, T. C., et al. (2000). The simulation of SST, sea ice extents and ocean heat transports in a version of the Hadley Centre coupled model without flux adjustments. *Climate Dynamics*, 16(2–3), 147–168. <https://doi.org/10.1007/s003820050010>
- Helama, S., Stoffel, M., Hall, R. J., Jones, P. D., Arppe, L., Matskovsky, V. V., et al. (2021). Recurrent transitions to little ice age-like climatic regimes over the Holocene. *Climate Dynamics*, 56(11–12), 3817–3833. <https://doi.org/10.1007/s00382-021-05669-0>
- Hopcroft, P. O., Kandlbauer, J., Valdes, P. J., & Sparks, R. S. J. (2018). Reduced cooling following future volcanic eruptions. *Climate Dynamics*, 51(4), 1449–1463. <https://doi.org/10.1007/s00382-017-3964-7>

- Jones, G. S., Gregory, J. M., Stott, P. A., Tett, S. F. B., & Thorpe, R. B. (2005). An AOGCM simulation of the climate response to a volcanic super-eruption. *Climate Dynamics*, 25(7–8), 725–738. <https://doi.org/10.1007/s00382-005-0066-8>
- Jungclauss, J. H., Fischer, N., Haak, H., Lohmann, K., Marotzke, J., Matei, D., et al. (2013). Characteristics of the ocean simulations in the Max Planck Institute Ocean Model (MPIOM) the ocean component of the MPI-earth system model. *Journal of Advances in Modeling Earth Systems*, 5(2), 422–446. <https://doi.org/10.1002/jame.20023>
- Klockmann, M., Mikolajewicz, U., Kleppin, H., & Marotzke, J. (2020). Coupling of the subpolar gyre and the overturning circulation during abrupt glacial climate transitions. *Geophysical Research Letters*, 47(21), e2020GL090361. <https://doi.org/10.1029/2020GL090361>
- Kobashi, T., Menviel, L., Jeltsch-Thömmes, A., Vinther, B. M., Box, J. E., Muscheler, R., et al. (2017). Volcanic influence on centennial to millennial Holocene Greenland temperature change. *Scientific Reports*, 7(1), 1441. <https://doi.org/10.1038/s41598-017-01451-7>
- Lehner, F., Born, A., Raible, C. C., & Stocker, T. F. (2013). Amplified inception of European little ice age by sea ice-ocean-atmosphere feedbacks. *Journal of Climate*, 26(19), 7586–7602. <https://doi.org/10.1175/JCLI-D-12-00690.1>
- Lin, J., Abbott, P. M., Sigl, M., Steffensen, J. P., Mulvaney, R., Severi, M., & Svensson, A. (2023). Bipolar ice-core records constrain possible dates and global radiative forcing following the ~74 ka Toba eruption. *Quaternary Science Reviews*, 312, 108162. <https://doi.org/10.1016/j.quascirev.2023.108162>
- Lohmann, J., Lin, J., Vinther, B. M., Rasmussen, S. O., & Svensson, A. (2024). State-dependent impact of major volcanic eruptions observed in ice-core records of the last glacial period. *Climate of the Past*, 20(2), 313–333. <https://doi.org/10.5194/cp-20-313-2024>
- Malmierca-Vallet, I., Sime, L. C., Valdes, P. J., Klockmann, M., Vettoretti, G., & Slaterry, J. (2024). The impact of CO₂ and climate state on whether Dansgaard-Oeschger type oscillations occur in climate models. *Geophysical Research Letters*, 51(13), e2024GL110068. <https://doi.org/10.1029/2024GL110068>
- Marshall, L. R., Maters, E. C., Schmidt, A., Timmreck, C., Robock, A., & Toohey, M. (2022). Volcanic effects on climate: Recent advances and future avenues. *Bulletin of Volcanology*, 84(5), 54. <https://doi.org/10.1007/s00445-022-01559-3>
- Mauritsen, T., Bader, J., Becker, T., Behrens, J., Bittner, M., Brokopf, R., et al. (2019). Developments in the MPI-M Earth system model version 1.2 (MPI-ESM1.2) and its response to increasing CO₂. *Journal of Advances in Modeling Earth Systems*, 11(4), 998–1038. <https://doi.org/10.1029/2018MS001400>
- Mehling, O., Bellomo, K., & von Hardenberg, J. (2024). Centennial-scale variability of the Atlantic meridional circulation. In *CMIP6 models shaped by Arctic-North Atlantic interactions and sea ice biases*. <https://doi.org/10.1029/2024GL110791>
- Metzner, D., Kutterolf, S., Toohey, M., Timmreck, C., Niemeier, U., Freundt, A., & Krüger, K. (2014). Radiative forcing and climate impact resulting from SO₂ injections based on a 200,000-year record of Plinian eruptions along the central American volcanic arc. *International Journal of Earth Sciences*, 103(7), 2063–2079. <https://doi.org/10.1007/s00531-012-0814-z>
- Mignot, J., Khodri, M., Frankignoul, C., & Servonnat, J. (2011). Volcanic impact on the Atlantic Ocean over the last millennium. *Climate of the Past*, 7(4), 1439–1455. <https://doi.org/10.5194/cp-7-1439-2011>
- Miller, G. H., Geirsdóttir, Á., Zhong, Y., Larsen, D. J., Otto-Bliesner, B. L., Holland, M. M., et al. (2012). Abrupt onset of the little ice age triggered by volcanism and sustained by sea-ice/ocean feedbacks. *Geophysical Research Letters*, 39(2), L02708. <https://doi.org/10.1029/2011GL050168>
- Model Development Team Max-Planck-Institut für Meteorologie. (2024). MPI-ESM 1.2.01p7 [Software]. *Edmond*. <https://doi.org/10.17617/3.H44EN5>
- Moreno-Chamarro, E., Zanchettin, D., Lohmann, K., & Jungclauss, J. H. (2017). An abrupt weakening of the subpolar gyre as trigger of little ice age-type episodes. *Climate Dynamics*, 48(3–4), 727–744. <https://doi.org/10.1007/s00382-016-3106-7>
- Myhre, G., Shindell, D., Bréon, F. M., Collins, W., Fuglestad, J., Huang, J., et al. (2013). Anthropogenic and natural radiative forcing. In *Climate change 2013: The physical science basis. Contribution of working group I to the fifth assessment report of the intergovernmental panel on climate change*. (Vol. 9781107057999). Cambridge University Press. <https://doi.org/10.1017/CBO9781107415324.018>
- Neukom, R., Barboza, L. A., Erb, M. P., Shi, F., Emile-Geay, J., Evans, M. N., et al. (2019). Consistent multidecadal variability in global temperature reconstructions and simulations over the common era. *Nature Geoscience*, 12(8), 643–649. <https://doi.org/10.1038/s41561-019-0400-0>
- Peltier, W. R., Argus, D. F., & Drummond, R. (2015). Space geodesy constrains ice age terminal deglaciation: The global ICE-6G-C (VM5a) model. *Journal of Geophysical Research: Solid Earth*, 120(1), 450–487. <https://doi.org/10.1002/2014JB011176>
- Pope, V. D., Gallani, M. L., Rowntree, P. R., & Stratton, R. A. (2000). The impact of new physical parametrizations in the Hadley Centre climate model: HadAM3. *Climate Dynamics*, 16(2–3), 123–146. <https://doi.org/10.1007/s003820050009>
- Reintges, A., Robson, J. I., Sutton, R., & Yeager, S. G. (2024). Subpolar North Atlantic mean state affects the response of the Atlantic meridional overturning circulation to the North Atlantic oscillation in CMIP6 models. *Journal of Climate*, 37(21), 5543–5559. <https://doi.org/10.1175/jcli-d-23-0470.1>
- Schleussner, C. F., & Feulner, G. (2013). A volcanically triggered regime shift in the subpolar North Atlantic Ocean as a possible origin of the little ice age. *Climate of the Past*, 9(3), 1321–1330. <https://doi.org/10.5194/cp-9-1321-2013>
- Sigl, M., Toohey, M., McConnell, J. R., Cole-Dai, J., & Severi, M. (2022). Volcanic stratospheric sulfur injections and aerosol optical depth during the Holocene (past 11 500 years) from a bipolar ice-core array. *Earth System Science Data*, 14(7), 3167–3196. <https://doi.org/10.5194/essd-14-3167-2022>
- SMIMIP, C., & Community, S. (2020). Arctic sea ice in CMIP6. *Geophysical Research Letters*, 47(10), e2019GL086749. <https://doi.org/10.1029/2019GL086749>
- Stevens, B., Giorgetta, M., Esch, M., Mauritsen, T., Crueger, T., Rast, S., et al. (2013). Atmospheric component of the MPI-M Earth system model: ECHAM6. *Journal of Advances in Modeling Earth Systems*, 5(2), 146–172. <https://doi.org/10.1002/jame.20015>
- Svensson, A., Dahl-Jensen, D., Steffensen, J. P., Blunier, T., Rasmussen, S. O., Vinther, B. M., et al. (2020). Bipolar volcanic synchronization of abrupt climate change in Greenland and Antarctic ice cores during the last glacial period. *Climate of the Past*, 16(4), 1565–1580. <https://doi.org/10.5194/cp-16-1565-2020>
- Svensson, A., & Lohmann, J. (2022). Ice core evidence for major volcanic eruptions at the onset of Dansgaard-Oeschger warming events. *Climate of the Past*, 18(9), 2021–2043. <https://doi.org/10.5194/cp-18-2021-2022>
- Timmreck, C. (2012). Modeling the climatic effects of large explosive volcanic eruptions. *Wiley Interdisciplinary Reviews: Climate Change*, 3(6), 545–564. <https://doi.org/10.1002/wcc.192>
- Timmreck, C., Graf, H. F., Lorenz, S. J., Niemeier, U., Zanchettin, D., Matei, D., et al. (2010). Aerosol size confines climate response to volcanic super-eruptions. *Geophysical Research Letters*, 37(24), L24705. <https://doi.org/10.1029/2010GL045464>
- Valdes, P. J., Armstrong, E., Badger, M. P. S., Bradshaw, C. D., Bragg, F., Crucifix, M., et al. (2017). The BRIDGE HadCM3 family of climate models: HadCM3@Bristol v1.0. *Geoscientific Model Development*, 10(10), 3715–3743. <https://doi.org/10.5194/gmd-10-3715-2017>

- van Dijk, E., Jungclauss, J., Lorenz, S., Timmreck, C., & Krüger, K. (2022). Was there a volcanic-induced long-lasting cooling over the Northern Hemisphere in the mid-6th-7th century? *Climate of the Past*, 18(7), 1601–1623. <https://doi.org/10.5194/cp-18-1601-2022>
- van Dijk, E. J. C., Jungclauss, J., Sigl, M., Timmreck, C., & Krüger, K. (2024). High-frequency climate forcing causes prolonged cold periods in the Holocene. *Communications Earth & Environment*, 5(1), 1–9. <https://doi.org/10.1038/s43247-024-01380-0>
- Willeit, M., Ganopolski, A., Edwards, N. R., & Rahmstorf, S. (2024). Surface buoyancy control of millennial-scale variations of the Atlantic meridional ocean circulation. *Climate of the Past*, 20(12), 2719–2739. <https://doi.org/10.5194/egusphere-2024-819>
- Yeager, S., & Danabasoglu, G. (2014). The origins of late-twentieth-century variations in the large-scale North Atlantic circulation. *Journal of Climate*, 27(9), 3222–3247. <https://doi.org/10.1175/JCLI-D-13-00125.1>
- Zanchettin, D., Bothe, O., Graf, H. F., Lorenz, S. J., Luterbacher, J., Timmreck, C., & Jungclauss, J. H. (2013). Background conditions influence the decadal climate response to strong volcanic eruptions. *Journal of Geophysical Research: Atmospheres*, 118(10), 4090–4106. <https://doi.org/10.1002/jgrd.50229>
- Zanchettin, D., Khodri, M., Timmreck, C., Toohey, M., Schmidt, A., Gerber, E. P., et al. (2016). The model intercomparison project on the climatic response to volcanic forcing (VolMIP): Experimental design and forcing input data for CMIP6. *Geoscientific Model Development*, 9(8), 2701–2719. <https://doi.org/10.5194/gmd-9-2701-2016>
- Zanchettin, D., Timmreck, C., Graf, H. F., Rubino, A., Lorenz, S., Lohmann, K., et al. (2012). Bi-decadal variability excited in the coupled ocean-atmosphere system by strong tropical volcanic eruptions. *Climate Dynamics*, 39(1–2), 419–444. <https://doi.org/10.1007/s00382-011-1167-1>
- Zhang, X., Lohmann, G., Knorr, G., & Purcell, C. (2014). Abrupt glacial climate shifts controlled by ice sheet changes. *Nature*, 512(7514), 290–294. <https://doi.org/10.1038/nature13592>
- Zhong, Y., Miller, G. H., Otto-Bliesner, B. L., Holland, M. M., Bailey, D. A., Schneider, D. P., & Geirsdottir, A. (2011). Centennial-scale climate change from decadal-paced explosive volcanism: A coupled sea ice-ocean mechanism. *Climate Dynamics*, 37(11–12), 2373–2387. <https://doi.org/10.1007/s00382-010-0967-z>

References From the Supporting Information

- Allan, R., & Ansell, T. (2006). A new globally complete monthly historical gridded mean sea level pressure dataset (HadSLP2): 1850–2004. *Journal of Climate*, 19(22), 5816–5842. <https://doi.org/10.1175/JCLI3937.1>
- Armstrong, E., Hopcroft, P. O., & Valdes, P. J. (2019). A simulated Northern Hemisphere terrestrial climate dataset for the past 60,000 years. *Scientific Data*, 6(1), 265. <https://doi.org/10.1038/s41597-019-0277-1>
- Cheng, J., Liu, Z., Zhang, S., Liu, W., Dong, L., Liu, P., & Li, H. (2016). Reduced interdecadal variability of Atlantic meridional overturning circulation under global warming. *Proceedings of the National Academy of Sciences of the United States of America*, 113(12), 3175–3178. <https://doi.org/10.1073/pnas.1519827113>
- de Boyer Montégut, C. (2024). Mixed layer depth over the global ocean: A climatology computed with a density threshold criterion of 0.03 kg/m³ from the value at the reference depth of 5 m. SEANOE. <https://doi.org/10.17882/98226>
- de Boyer Montégut, C., Madec, G., Fischer, A. S., Lazar, A., & Iudicone, D. (2004). Mixed layer depth over the global ocean: An examination of profile data and a profile-based climatology. *Journal of Geophysical Research*, 109(12), C12003. <https://doi.org/10.1029/2004JC002378>
- Good, S. A., Martin, M. J., & Rayner, N. A. (2013). EN4: Quality controlled ocean temperature and salinity profiles and monthly objective analyses with uncertainty estimates. *Journal of Geophysical Research: Oceans*, 118(12), 6704–6716. <https://doi.org/10.1002/2013JC009067>
- Gowan, E. J., Zhang, X., Khosravi, S., Rovere, A., Stocchi, P., Hughes, A. L. C., et al. (2021). A new global ice sheet reconstruction for the past 80 000 years. *Nature Communications*, 12(1), 1199. <https://doi.org/10.1038/s41467-021-21469-w>
- Kageyama, M., Harrison, S. P., Kapsch, M. L., Lofverstrom, M., Lora, J. M., Mikolajewicz, U., et al. (2021). The PMIP4 last glacial maximum experiments: Preliminary results and comparison with the PMIP3 simulations. *Climate of the Past*, 17(3), 1065–1089. <https://doi.org/10.5194/cp-17-1065-2021>
- Köhler, P., Knorr, G., Buiron, D., Lourantou, A., & Chappellaz, J. (2011). Abrupt rise in atmospheric CO₂ at the onset of the Bølling/Allerød: In-situ ice core data versus true atmospheric signals. *Climate of the Past*, 7(2), 473–486. <https://doi.org/10.5194/cp-7-473-2011>
- Prange, M., Jonkers, L., Merkel, U., Schulz, M., & Bakker, P. (2023). A multicentennial mode of North Atlantic climate variability throughout the last glacial maximum. *Science Advances*, 9(44), eadh1106. <https://doi.org/10.1126/SCIADV.ADH1106>
- Rehfeld, K., Hebert, R., Lora, J. M., Lofverstrom, M., & Brierley, C. M. (2020). Variability of surface climate in simulations of past and future. *Earth System Dynamics*, 11(2), 447–468. <https://doi.org/10.5194/esd-11-447-2020>
- Rehfeld, K., Münch, T., Ho, S. L., & Laepple, T. (2018). Global patterns of declining temperature variability from the last glacial maximum to the Holocene. *Nature*, 554(7692), 356–359. <https://doi.org/10.1038/nature25454>
- Tierney, J. E., Zhu, J., King, J., Malevich, S. B., Hakim, G. J., & Poulsen, C. J. (2020). Glacial cooling and climate sensitivity revisited. *Nature*, 584(7822), 569–573. <https://doi.org/10.1038/s41586-020-2617-x>